LATVIAN JOURNAL OF PHYSICS AND TECHNICAL SCIENCES
2005, N 1

RADIATION-INDUCED CONDUCTIVITY IN INORGANIC DIELECTRIC MATERIALS

U. Ulmanis, N. Mironova-Ulmane

Institute of Solid State Physics, University of Latvia,
Kengaraga iela 8, Riga, LV-1063, LATVIA
ulman@latnet.lv

The radiation-induced electrical conductivity (RIC) of MgO, GGG, alumina and TeO_2 single crystals and Eu_2O_3 ceramic inorganic materials was studied under irradiation in the IRT fission reactor at temperatures 20–400 °C with the gamma-ray dose rates of 10^2–10^5 Gy/h and the neutron fluxes of 10^9–10^{12} n/cm^2·s. The RIC variation with dose rate follows the power law with a dose rate exponent 0.67–1.0. During the irradiation a decrease in the activation energy of electric conductivity of irradiated specimens was observed.

1. INTRODUCTION

The present work is a contribution to the understanding of important electrical transport processes in the single crystals and ceramic dielectric materials, such as alumina, magnesia, tellurium and europium oxides, etc., at different temperatures under gamma-neutron irradiation. Transport processes in insulating solid materials with low conductivity are of considerable technological interest, since they are often the controlling factors determining important properties and use of a material at high temperatures in ionising fields. Dielectric oxide materials are expected to play the crucial role under gamma-neutron irradiation in fission and fusion reactors. Among the effects exerted by irradiation on electrical properties the increase in the electric conductivity as a result of electronic excitation and ionisation can be mentioned – the well-known effect of radiation-induced conductivity (RIC) in dielectric materials. To this effect in different dielectric materials a great body of literature data is devoted [1–6]. The RIC phenomenon is a complicated dynamic process which involves interaction among various defects and electric charge carriers. The electric conductivity during irradiation may be expressed as the empirical relation

$$\sigma = \sigma_0 + \sigma_\rho = \sigma_0 + KP^d, \qquad (1)$$

where σ_0 is the conductivity in the absence of irradiation, and σ_r is the radiation-induced conductivity or RIC. The value of σ_0 depends on the temperature, crystal structure, purity, defectiveness, ambient gases and contact resistance. In turn, the RIC depends on the radiation type, energy, dose rate, fluence, as well as on the temperature during irradiation. In (1) the term P is the ionising dose rate, and K, d are constants. It is known that these constants depend on the irradiation temperature, dose rate and material defectiveness [5–10]. For example, the value of d (the radiation dose rate exponent) for alumina, which can be directly obtained from the experimental curve, is a complex function of temperature [5]. In the proximity of room temperature d = 0.7–0.9, and with the temperature increasing it decreases to its minimum of 0.5. The temperature corresponding to this minimum increases with dose rate increasing [5]. For MgO d = 0.9–1.1, in which case the temperature dependence is also observed [7]. For polycrystalline Al_2O_3 Pells [8] found that $d > 1.0$. In

the case of $MgAl_2O_4$ it was revealed that this parameter may be dose-dependent itself [10]. The value of d is generally between 0.5 and 1.0, which means a quasi-continuum of discrete energy states in the forbidden band and is determined by a balance between the production of free charge carriers by ionisation, their trapping at different centres and recombination of electron-hole pairs. For $d \sim 1.0$ (homogenous distribution of the trapping centres) a weak temperature dependence and for $d = 0.5$ (exponential distribution) – a stronger temperature dependence for RIC is observed. As trapping centres in dielectric materials there serve impurities, structural defects and dislocations.

The value of proportionality constant K strongly depends on the material, with typical RT values ranging from 10^{-12} to 10^{-9} $(Sm^{-1})/(Gy \cdot \cdot s^{-1})$ [3].

The insulating materials in fusion reactors are influenced by the electric field, elevated temperatures and radiation. These conditions are abbreviated as RET (**R**adiation - **E**lectric Field - **T**emperature) [11]. In recent years the RIC investigations of Hodgson *et al.* [9] in dielectric ceramic and single crystal materials at elevated temperatures (250–900 °C), moderate electric field (> 20 kV/m) and radiation damage (> 10^{-5} dpa) have shown a new – entirely unforeseen – effect: the constant saturation level of RIC is not maintained, with this conductivity exhibiting in some cases a sharp increase up to 2–3 orders of magnitude. This phenomenon was named radiation - induced electrical degradation (RIED). From the results of extended experiments by Hodgson, Pells, Shikama, Zinkle *et al.* [4, 9, 12–14] it is seen that this effect depends on the temperature, electric field, material, dose rate and irradiation time. The RIED shows considerable promise for application in fusion or fission reactors since in most applications of dielectrics as nuclear energy materials the electrical conductivity during irradiation must be less than 10^{-4} S/m .

In [14] Hodgson explains the RIED effect by solid-state radiolysis in alumina during irradiation under the RET conditions. He observed the formation of aluminium colloids similar to that typical of colloid production in alkali halides. This hypothesis relies upon the idea that under the RET conditions in alumina more mobile F^+ centres are predominantly generated as compared with F-centres generated in the absence of these conditions. A large team of scientists from USA, China, and other countries has proposed another hypothesis – that the RIED effect is caused by dislocations generated during irradiation [11]. It should be noted that there are also experiments that show no RIED effect (see review [6]). It is becoming increasingly clear that the problem of choosing electrically insulating materials for future reactors is far more serious than initially anticipated. The chosen materials - refractory oxides or ceramics - will have to keep their high electrical resistivity, thermal conductivity, mechanical strength , and dielectric properties during prolonged irradiation.

In the present work we studied the RIC under irradiation in a fission reactor for differently structured crystals: MgO, α- Al_2O_3, $Gd_3Ga_5O_{12}$ (GGG), TeO_2 and Eu_2O_3. As concerns TeO_2 and Eu_2O_3 crystals, this is for the first time that the steady-state RIC has been studied over a wide range of temperatures and dose rates. It is known that the structure of these materials plays a major role not only in the radiation defect generation but also in the defect kinetics. Some of our experimental results for MgO, α-Al_2O_3 and GGG are presented in [15], for ceramic AlN – in [16] and for ceramic ferroelectrics - in [17].

2. EXPERIMENTAL PROCEDURE

As the radiation source a horizontal experimental channel (10 cm in diameter, 280 cm long) of the Latvian IRT 5 MW water-water research reactor was used, with the known gamma-neutron dose rate distribution along its length measured with a gamma-dosimeter and neutron activation monitors. The irradiation facility provides for moving the holder with a furnace, samples and measuring cables into the active core of the reactor, and for keeping the sample at any distance from the active core for the time required, thus changing the radiation dose rate by three orders (1 kGy/h – 1 MGy/h, 10^9–10^{12} $n/cm^2 \cdot s$ [18] (Fig. 1).

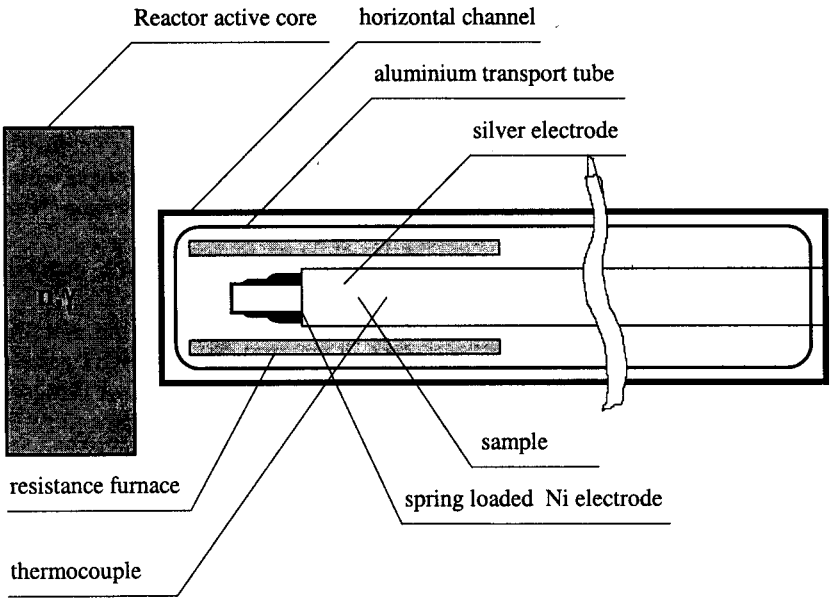

Fig. 1. Schematic illustration of the irradiation system for in-situ measurements of electric conductivity

As samples we used MgO, GGG, alumina and TeO_2 single crystals, and Eu_2O_3, AlN and ferroelectric ceramics with dimensions (5–10)×(4–8)×(0.5–3.0) mm^3. The MgO sample employed in this work was grown by the arc-fused technique. The neutron activation analysis for impurity content showed ~ 10^{-3} at. % of iron group metals in the sample (so far, no data have been available as to the content of impurities in other crystals).

In microelectronics, alumina and GGG are widely used as substrate materials. For GGG crystals the density of dislocations is known to be greater than 10 cm^{-2}. The AlN powder was produced at the Latvian Institute of Inorganic Chemistry [16].

The samples with measuring cables were placed in the resistance furnace, allowing the temperature up to 500 °C to be kept during irradiation. The temperature of the samples was measured in-situ, with a chromel-alumel thermocouple inserted in a heater 2–3 mm behind the sample. In this case some difference arises between the thermocouple data and the sample temperature depending on the heating rate.

The samples had two thermally-deposited silver electrodes, each sample having the form of a sandwich with a crystal between two flat spring-loaded nickel electrodes for applying electric field to the sample.

The electric resistivity of the samples was measured in the air, by the conventional d.c. two-terminal method.

There are some peculiarities in measuring the electro-physical parameters of materials during irradiation stemming from the radiation-induced changes in the surrounding medium, construction materials and measuring detectors. The in-situ measurements in nuclear reactors usually involve many technical problems. Intense radiation field in the reactor ionises the air around the sample. As a result, the electrical insulation of the sample will deteriorate, and a parasitic electric current will be generated, which may disturb the measurements. Analysis of the in-situ electrical measurements in radiation fields is given in [19–23]. Summary conclusions are given by Evans [6]. They read as follows "... future evaluations must employ three-terminal network, the origins of surface contamination need to be guarded against, guard ring electron contact resistance monitored and kept appropriately low, and surface clearness between guard ring and central electrode confirmed." In

our case, owing to experimental restrictions, the guard ring technique and the vacuum system could not be applied for suppression of the influence of surface. Since we had no guard ring and the conductivity was measured in air, some stray leakage currents might give additional conductivity, therefore the resulting pre- and post-irradiation conductivity values at low temperatures can be used for qualitative comparison only. A similar situation is discussed in work [11], the authors of which also used two-terminal d.c. electrodes in air under assumption that the surface current was very small as compared with the RIC owing to oxidation of surface impurities and could therefore be neglected.

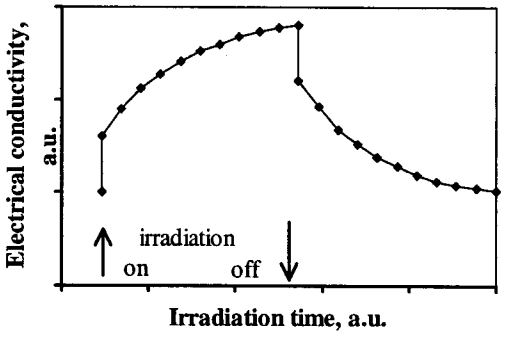

Fig. 2. Radiation-induced electrical conductivity of ceramic insulating material *vs.* irradiation time

Additional experiments were carried out to account for polarisation effects and time dependence at conductivity measurements. When voltage is applied the conductivity does not remain constant but is slowly growing up to a given value. To reduce the influence of these effects on the reliability of conductivity measurements, they were performed using one value of the measuring voltage. After the irradiation was terminated, the RIC of the sample did not disappear instantaneously – but, instead, the initial RIC fall was soon followed by a slow and gradual decrease (see Fig. 2). This picture, having repeated after each step-by-step change of the dose rate, had to be taken into account when studying the conductivity - dose rate dependence.

3. RESULTS AND DISCUSSION

The measured d.c. conductivity in the reactor's gamma-neutron field is influenced both by temperature and by ionisation dose rate. Figure 3 shows the influence of temperature on the electrical conductivity before and during irradiation in single crystals TeO_2, and ceramic Eu_2O_3; as usual, the ordinate presents the electric conductivity plotted on the logarithmic scale as a function of the absolute temperature reciprocal. The experimental results – the activation energy before and during irradiation, RT conductivity and *d, K* constants are given in Table 1. The electric conductivity of MgO before radiation has activation energy 1.43 eV above 230 °C and is weakly dependent on temperature below this value. At low temperatures (much lower than the melting temperature), in contrast with the electric conductivity behaviour at melting temperatures (for our crystals ~ 500 °C), the electric conductivity is not clearly expressed. This could be explained with the fact that the measurements of insulating materials below 500 °C are always complicated by the prehistory of a sample (impurities, structure defects) as well as by the experimental technique used, in particular, for the in-situ distant measurements. The low activation energy in the temperature region from RT up to 500 °C (0.5–1.2 eV in the region of 150–500 °C) allows us to conclude that at low temperatures in MgO, Al_2O_3, GGG, TeO_2 and Eu_2O_3 the electron

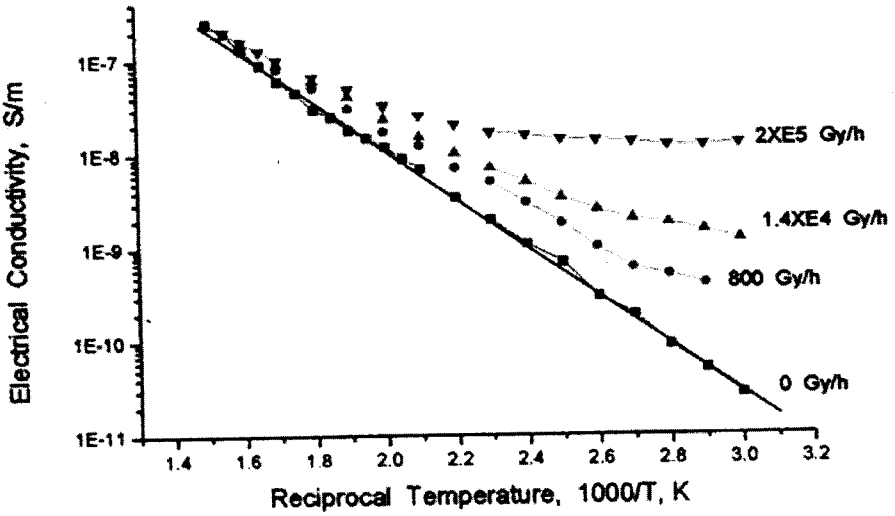

Fig. 3. Electrical conductivity of TeO_2 as a function of reciprocal temperature at different gamma-rays dose rates

(hole) mechanism of conduction prevails, associated with the energy levels of impurities and defects in the forbidden band. The magnitudes of the observed conductivity and activation energy are almost the same as the reported values of intrinsic conductivity and activation energy in MgO [7], alumina [4], GGG [24], paratellurite [25] and Eu_2O_3 [26]. However, convincingly enough, these results are interesting only for comparison with radiation-induced changes in the electric conductivity, and they do not allow any data to be obtained about the mobility of charge carriers and their trapping and de-trapping centres. The effect of thermal cycling on the intrinsic conductivity for AlN is reported in [16]. A strong influence of surface conditions on the results could be clearly seen. For example, in the temperature region from RT to 100–130 °C hysteresis of the conductivity can be observed. Thermal cycling performed at these temperatures reduces the conductivity, which is probably connected with changes in the surface conditions (contaminations, moisture, etc.). Our results for the intrinsic conductivity in Figs. 3–5 relate to the experiments after the second thermal cycling. The measurements of electric conductivity *vs.* the reciprocal temperature for GGG performed with and without a guard ring evidence a similar behaviour of conductivity in the temperature region below 100 °C [24].

Table 1

Conductivity characteristics for differently structured crystals: RT conductivity (σ_0), activation energy of intrinsic conductivity (E_a), RIC at 800 Gy/h, activation energy of RIC (E_{ar}), dose rate exponent (d), proportionality constant (K)

Crystal	Structure	σ_0, S/m	E_a, eV	RIC, S/m	E_{ar}, eV	d	K, $(S\cdot m^{-1})/(Gy\cdot s^{-1})$
MgO	rocksalt	10^{-13}	1.22	$2\cdot10^{-11}$	0.6	0.63	$3\cdot10^{-9}$
Al_2O_3	corundum	$2\cdot10^{-12}$	0.72	$2.5\cdot10^{-10}$	0.18	0.7	$2.4\cdot10^{-10}$
$Gd_3Ga_5O_{12}$	garnet	$1.2\cdot10^{-12}$	0.5	$5\cdot10^{-11}$	0.33	0.67	$1.4\cdot10^{-10}$
TeO_2	rombic	$9\cdot10^{-11}$	0.54	$5\cdot10^{-10}$	0.38	0.67	$1.4\cdot10^{-9}$
Eu_2O_3	cubic C	$5\cdot10^{-12}$	0.94	$5\cdot10^{-10}$	0.8	1.0	$2.2\cdot10^{-9}$

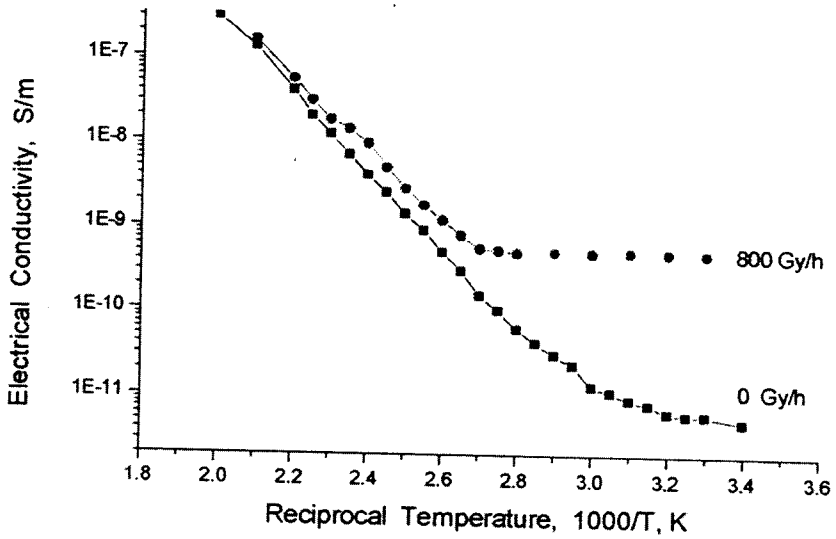

Fig. 4. Electrical conductivity of Eu_2O_3 as a function of reciprocal temperature at different gamma-ray dose rates

During irradiation, the activation energy of MgO decreases to 0.66 eV at 600 Gy/h and to 0.33 eV above 160 °C at 300 kGy/h, and is practically independent of temperature with the activation energy of 0.1–0.2 eV below 150 °C. Similar results have been obtained also for Al_2O_3, GGG, TeO_2 and Eu_2O_3 (see Figs. 3, 4 and [15]). The temperature dependence of the RIC for MgO and alumina shows a reasonable agreement with the results for MgO and alumina reported previously [4, 7]. Figure 5 shows a typical result for electric conductivity as a function of the gamma dose rate in the reactor for MgO, alumina, GGG, Teo_2 and Eu_2O_3 irradiated at 60–200 °C in the log-log plot. In this figure, the straight-line fit to the data points in this temperature range shows that the RIC variation with gamma-dose rate follows a power law with the dose rate exponent d = 0.67–1.0 and the proportionality constant $K = 10^{-9}$–10^{-12} $(S \cdot m^{-1})/(Gy \cdot h^{-1})$ (see Table 1). At higher temperatures the results are more complex, and the RIC values become comparable with the intrinsic conductivity. The measurements show also a hysteresis in the RIC values depending on the dose rate (increased or decreased) and on the irradiation time. Concerning the d parameter, so far its dependences – e.g. on the temperature and dose rate – have not been obtained.

The effect of gamma-neutron irradiation consists in the production of electron-hole pairs by transfer of excited electrons from the valence band to the conduction band, the change in the concentration of charge carriers in trapping and de-trapping centres, and the generation of point – and more complex - radiation defects. For our samples the effect of nuclear reactions may be ignored. As compared with the authors of [19, 20, 27, 28] who used the neutron radiation with knocking-on the atoms produced by the elastic scattering of fast neutrons, in our experimental conditions of gamma irradiation the generation rate of charge carriers is one-two orders of magnitude higher. The radiation-induced conductivity value is determined mainly by the generation rate of charge carriers, their trapping and thermal de-trapping, as well as by the recombination rate of free electrons and holes. It should be noted that radiation induces hot charge carriers (those with a high kinetic energy, such as Compton and photoelectrons with the maximum energy close to that for gamma-rays). Both the electrons and the holes thermalise and begin to diffuse under the applied electric field. Thus the RIC effect is predominantly associated with ionisation processes.

Obviously enough, long-term irradiation can change the character and concentration of trapping centres and thus to affect the RIC. The general aspects of the RIC behaviour could be explained by the multitrap photoconductivity theory.

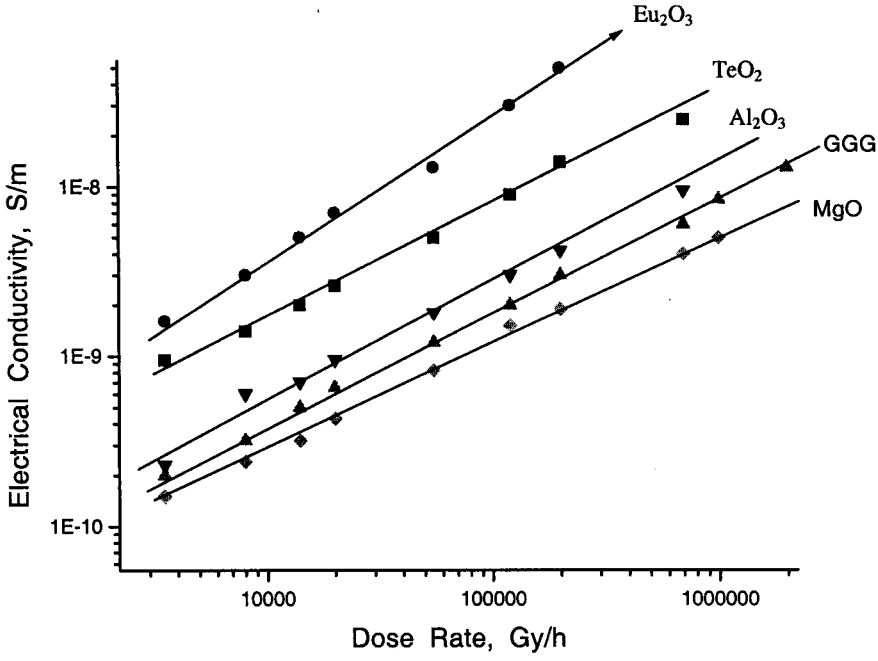

Fig. 5. Electrical conductivity of insulating materials *vs.* gamma ray dose rate

To calculate the RIC theoretically, the continuity equation can be used [5]:

$$dn/dt = g - g_t + g_d - g_r, \tag{2}$$

where the generation rate of charge carriers (electrons) $g = P/w$ is the ratio between the dose rate P absorbed by the material and the energy w necessary for the creation of an electron-hole pair.

For dielectric crystals the relationship $w = 3E_a$ can be used, where E_a is the optical band gap, g_t is the carrier trapping rate, g_d is the carrier de-trapping rate, and g_r is the carrier recombination rate. A similar equation holds for holes. For the samples with the known equation for the trapping and de-trapping centres (see Eq. (2)) the analysis allows for evaluation of the properties of the radiation-induced conductivity. As an example, a simple two-trap model for Al_2O_3 has been analysed by Klaffky *et al.* [5], who assumed the mobility of electrons to be 1 $cm^2 \cdot V^{-1} \cdot s^{-1}$, which is some orders of magnitude greater than that of holes. The increase in the RIC observed at the increasing temperature was explained by the thermal release of electrons from shallow and deep electron traps, while the decrease in the RIC - by the thermal release of trapped holes followed by quenching the conductivity through the recombination of holes with electrons at the shallow electron traps.

4. CONCLUSION

During our studies carried out in a wide range of oxide insulators no basic differences were revealed in the experimental results obtained for the RIC of different materials, which are qualitatively similar. The temperature dependence of conductivity

before and during irradiation is similar for the samples with different crystal structure. In the studied insulating materials the RIC increases with the reactor gamma dose rate and in a first approximation obeys the conventional power law describing its dependence on the ionising dose rate.

REFERENCES

1. Clinard F.W Jr. and Hobs L.W (1986) in: *Physics of Radiation Effects in Crystals* (eds. R.A. Johnson and A.N. Orlov) Amsterdam: Elsevier, p. 387.
2. Kostyukov N.S., Muminov M.I., Kim Gen-Tschan, Oxengendler B.L., Skripnikov Yu.S. (1986) *Radiation Effects in Ceramic Insulators* (in Russian) Tashkent: FAN, p.67.
3. Zinkle S.J and Hodgson E.R. (1992) *J. Nucl. Mater.* **191–194** 58.
4. Pells G.P. (1994) *J. Am. Ceram. Soc.* **77[2]** 368.
5. Klaffky R.W, Rose B.H, Goland A.N and Dienes G.J (1980) *Phys. Rev.* B **21** 3610.
6. Evans B.J. (1995) *Nucl. Mater.* **219** 202.
7. Hodgson E.R and Clement S. (1988) *J. Nucl. Mater.* **152** 357.
8. Pells G.P (1986) *Radiat. Eff.* **97** 199.
9. Hodgson E.R (1989) *Cryst. Latt. Def. and Amorph. Mater.* **181** 69.
10. Pells G.P. (1991) *J. Nucl. Mater.* **184** 183.
11. Zong H.-F., Shen C.-F., Liu S., Wu Z.-C., Chen Yi., Chen Y., Evans B.D., Gonzalez R. and Sellers C.H. (1994) *Phys. Rev.* b **49** 15514.
12. Shikama T., Narui M., Endo Y., Sagawa T. and Kayano H. (1992) *J. Nucl. Mater.* **191–194** 575.
13. Kinoshita Ch. and Zinkle S.J. (1996) *J. Nucl. Mater.* **233–237** 100.
14. Hodgson E.R. (1991) *J. Nucl. Mater.* **179–181** 383.
15. Ulmanis U. (1997) in: *Optical Organic and Semiconductor Inorganic Materials* (eds. E. Silinsh, A. Medvid, A. R.Lusis, A. O.Ozols) *Proc. SPI* **2967** 96–100.
16. Ulmanis U., Palcevskis E. (1998) *J. Nucl. Mater.* **252** 195–199.
17. Sternberg A., Spule A., Shebanovs L., Birks E., Kulis P., Weber H.W., Sauerzopf F.M., Klima H. and Ulmanis U. (1997) in: *Optical Organic and Semiconductor Inorganic Materials* (eds. E. Silinsh, A. Medvid, A.R. Lusis, A.O. Ozols) *Proc. SPI* **2967** 186–192.
18. Dinduns S.S, Lapenas A.A and Ulmanis U.A. (1983) *Horizontal Experimental Channels of Reactor IRT in Radiation Physics Research* (in Russian) *Preprint* LAFI – 056, Latv. Inst. of Phys., Salaspils (Latvia) 49 p.
19. Kostyukov N.S., Antonova N.P and Zilberman M.I (1979) *Radiation Material Science* (in Russian) Moscow: Atomizdat, p. 161.
20. Farnum E.H. and Clinard Jr.F.W. (1995) *J. Nucl. Mater.* **219** 161.
21. Kesternich N., Scheuermann F. and Zinkle S.J. (1993) *J. Nucl. Mater.* **206** 68.
22. Jung P., Zhu Z and Klein H. (1993) *J. Nucl. Mater.* **206** 72.
23. Narui M., Shikama T., Endo Y., Sagawa T., Kayamo H. (1991) *J. Nucl. Mater.* **191–194** 592.
24. Hartman E., Kovacs L. and Paitz J. (1984) *Phys. Stat. Sol.* (a) **86** 401.
25. Hartman E., Kovacs L. (1982) *Phys. Stat. Sol.* (a) **59** 59.
26. Samohvalov A.A., Bamburov V.E., Volkenstein N.V. (1966) *Izvestiya Akademii nauk SSSR* ser. Fizicheskaya (in Russian) **52** 984.
27. Alekseevskii O.B.,Vorobiev S.A and Kostyukov N.S. (1988) *Phys. Stat. Sol.* (b) **146** (2) K 109.
28. Itoh N., Tanaka T.and Clinard F.W. (1991) *J. Nucl Mater.* **183** 25.

RADIĀCIJAS INDUCĒTĀ VADAMĪBA DAŽOS NEORGANISKOS DIELEKTRISKOS MATERIĀLOS

U. Ulmanis, Ņ. Mironova – Ulmane,

K o p s a v i l k u m s

Magnija oksīda, korunda, gallija-gadolīnija granāta, tellura oksīda monokristālu un keramiska eiropija oksīda radiācijas inducētā vadamība (RIV) mērīta ar reaktora IRT gamma-neitronu plūsmu apstarotos paraugos apstarošanas laika temperatūru intervālā no 20 līdz 400 °C. Šo materiālu RIV pieaug ar starojuma dozas jaudu un dozas jaudas eksponente ir 0,67–1,0. Pie dozas jaudas lielākas par 10^5 Gy/h elektrovadamība nav atkarīga no temperatūras. Apstarošanas laikā elektrovadamības aktivācijas enerģija samazinās.

11.02.2005.